A Wearable Electrostatic Sensor for Human Activity Monitoring

Yonghui Hu, *Senior Member*, *IEEE*, and Yong Yan, *Fellow, IEEE*

***Abstract*—Human activity monitoring based on wearable sensors is important in a wide range of biomedical and healthcare applications. Existing wearable sensors using a single unit cannot capture the movements of all body segments. This paper presents a novel wearable electrostatic sensor that can detect limb and torso movements during routine daily activities from any location on the body. Because the electric potential of the human body varies during movements, the sensor measures the potential difference between the body and the electrode for motion sensing. A charge amplifier converts the induced charge on the electrode into a voltage signal, which is further amplified, filtered, digitalized and transmitted via ZigBee. Experimental assessment was carried out by collecting sensor signals from three locations simultaneously while the subject performing different movements. The capability of the sensor to capture limb and torso movements from any location is validated. The characteristics of the sensor are quantified by correlating the sensor signal to simple and cyclic movements. It is found that the sensor signal depends on the sensor's mounting location on the body, the type of activity and various factors.**

***Index Terms*—Wearable sensor, electrostatic sensor, human activity monitoring, capacitive coupling, charge amplifier.**

I. Introduction

HUMAN physical activities refer to any form of body movements produced by the contraction of skeletal muscles. Monitoring of human physical activities aims to provide information on various types of actions and behaviors in real-world settings. Such information is useful in a wide range of applications, such as quantitative health assessment [1], fall detection and prevention [2], sport movement analysis [3], human-machine interaction [4], among many others.

Significant research efforts have been undertaken in the last decade to develop sensing techniques for human activity monitoring. Existing techniques can be broadly classified into two categories, namely ambient and wearable [5]. Ambient sensors are embedded into the daily living environment and unobtrusively detect environmental changes caused by human activities, such as temperature, light, sound, pressure, etc [6]. Ambient assisted living systems utilize such sensors to monitor the well-being of individuals in the living environment [7]. Ambient sensors have limited coverage area and suffer from poor accuracy and low spatial resolution of activity recognition. Video cameras, as the most common ambient sensors, raise wide privacy and security concerns. By contrast, wearable sensors attached to various parts of the human body can overcome the above drawbacks. Inertial sensors, including accelerometers and gyroscopes, are most widely used for movement detection and tracking [8]. Magnetometers are often used in combination with inertial sensors for improved motion tracking. Current MEMS (Micro-Electro-Mechanical-Systems) technology has enabled miniaturization, mass production, and cost reduction of motion sensors, making them highly attractive for human activity monitoring applications. Foot pressure sensors embedded into insoles has been used to monitor ambulatory movements [9]. Since muscle contraction generates electrical signals called electromyography (EMG), detection of EMG signals using rigid or textile electrodes also enables monitoring of human activities [10]. Although wearable sensors allow long-term continuous monitoring of human activities in a free-living environment, there are still many limitations on the capacity of existing sensors in view of the diverse range of applications. For instance, a single wearable sensor cannot cover the entire body and fails to capture the movements of body segments that have no sensors attached to. Unreliable or erroneous results are inevitable for activity volume assessment or recognition due to undetected movements.

A network of wearable sensors spatially distributed over the human body can address the above problem. However, such a system, known as Wearable Body Area Network (WBAN), is complex, expensive and power hungry, in comparison with a single sensor. This paper presents a novel wearable electrostatic sensor capable of detecting limb and torso movements during routine daily activities with the sensor placed at any location on the body. The sensor works on the principle that variation of the capacitive coupling between the naturally charged human body and the environment during body movements leads to change in body potential [11]. Because the human body is a good conductor, potential variation caused by one body segment is detectable from elsewhere on the body.

Monitoring of human activity using electrostatic sensors has been studied in a few previous publications, in which different terms such as electric potential sensor and capacitive sensor have been used to describe the same technique. Kurita and Morinaga employed an electrode placed several meters away to

Manuscript received Month xx, 20xx; revised Month xx, 20xx; accepted Month xx, 20xx.. (*Corresponding author: Yonghui Hu*)

Y. Hu is with the School of Control and Computer Engineering, North China Electric Power University, Beijing 102206, China (phone: 86-10-61772893; e-mail: huyhui@gmail.com).

Y. Yan is with the School of Engineering, University of Kent, Canterbury, Kent CT2 7NT, UK (e-mail: y.yan@kent.ac.uk).

detect the change in the electric potential of the human body performing daily activities, including walking [12], standing up from and sitting down on a chair [13]. Li *et al*. measured the temporal gait parameters using the induced current on an electrode located 3 m away from walking subjects [14]. Kim and Moon used four electric potential sensors fixed at the corners of a TV screen to detect the electric disturbance due to moving hands for gesture recognition [15]. Tang *et al*. developed a triboelectric touch-free screen sensor for smartphones capable of recognizing diverse hand gestures by utilizing the charges naturally carried on the human body [16]. Tang and Mandal measured the respiration activity of a stationary subject using an electric potential sensor located 0.5 m away [17]. Indoor human localization based on passive electric field sensing has also been investigated by Tang and Mandal [17], Grosse-Puppendahl *et al*. [18], and Prance *et al*. [19]. It is notable that in the above studies the electrostatic sensors were fixed in the environment or on smart devices, operating in ambient mode. The primary limitations of ambient electrostatic sensors for human activity monitoring lie in short sensing range and strong dependence of the signal strength on the distance between the body and the electrode.

The idea of wearable electric field sensing was first proposed by Cohn *et al*. [20], who realized movement detection by measuring the capacitive coupling between the body and the environment. Later, Pouryazdan *et al.* used an electric potential sensor worn on the wrist to detect hair touch and leg movements [21]. The sensors developed by Cohn *et al*. and Pouryazdan *et al.* are both powered by batteries and use wireless transceivers for data logging, because wired connections to a DC power supply or a data acquisition device change the ground reference of the sensor circuit and significantly increase the signal strength, according to our experimental results. The major difference between the two sensors lies in their implementations, with the sensor in [20] requiring an electrode in direct contact with the skin, while the sensing electrode in [21] pointing away from the body. Because the sensor can work in ambient mode, the outward-pointing electrode is readily affected by nearby moving subjects.

In contrast to the design in [20], the wearable electrostatic sensor presented in this paper does not require the electrode to be in direct contact with the skin, thus offering numerous advantages. For instance, it avoids skin irritations due to metal allergies. Cloth is allowed to be present between the electrode and the skin, thus providing more flexibility in deployment, although the signal strength depends on the thickness and permittivity of the cloth. In addition, in comparison with the outward-pointing electrode in [21], an electrode pointing toward the body can achieve higher sensitivity and fidelity as well as enhanced immunity to interference in body potential measurement.

It is worth noting that non-contact capacitive sensors have been widely used to collect human electrophysiological signals, such as EMG, ECG (Electrocardiography) and EEG (Electroencephalography) [22]. Movement of the human body during electrophysiological recording causes strong interference which is referred to as motion artifact [23]. It is exactly the unwanted motion artifact caused by human movement that is used in this study for activity monitoring.

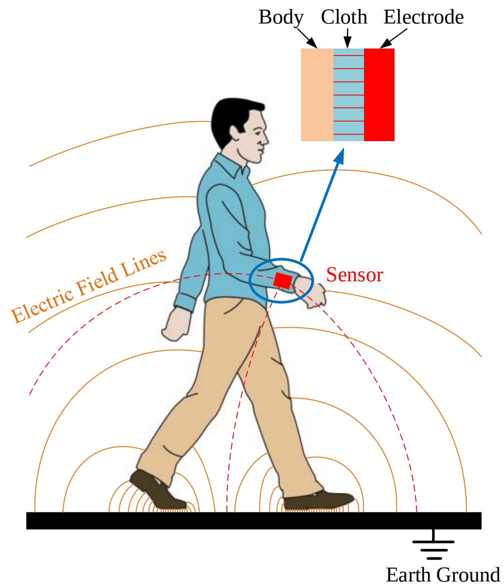

Fig. 1. Capacitive coupling among the human body, the sensor and the earth ground.

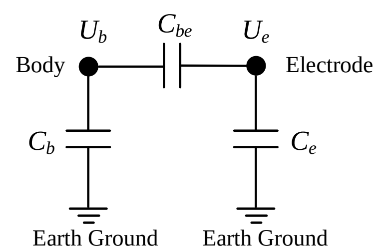

Fig. 2. Equivalent circuit model.

II. Sensing Principle and Sensor Design

A. Sensing Principle

Triboelectric charging is a ubiquitous phenomenon. When performing daily activities such as walking on insulated floors and taking off clothes, the human body becomes electrostatically charged. As the charge builds up on the body, high electric potential develops with reference to the earth ground with zero potential [24]. In an indoor environment, the building made of ferroconcrete acts as the earth ground. The body movements cause changes in the distance and thus capacitive coupling between the body and the earth ground, which further leads to variation of the body potential.

When the electrostatic sensor is worn on the wrist with cloth between the electrode and the skin, there exists capacitive coupling among the body, the electrode and the earth ground, as indicated with electric field lines in Fig. 1. The sensing system can be described using an equivalent circuit model consisting of lumped capacitors, as shown in Fig. 2. The body is capacitively coupled to the earth ground through C_b. The electrostatic sensor is battery-powered, and the electrode is held at the local ground potential. The electrode and the local ground plane are capacitively coupled to the earth ground through C_e. Additionally, the capacitive coupling between the body and the

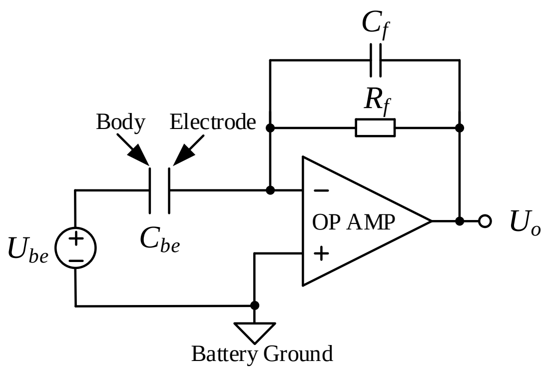

Fig. 3. Circuit diagram of the charge amplifier.

electrode is denoted using C_{be}. The electrostatic sensor measures the potential difference U_{be} between the body and the electrode, which is expressed as

$$\begin{aligned} U_{be} &= U_b - U_e \\ &= \frac{Q_b}{C_b} - \frac{Q_e}{C_e} \end{aligned} \tag{1}$$

where U_b and U_e are the potential of the body and the electrode, respectively, and Q_b and Q_e are the net charges on the body and the electrode, respectively.

When the electrostatic sensor is firmly attached to the body, the capacitance C_{be} remains constant. It can be seen from equation (1) that changes in the charges Q_b and Q_e as well as changes in the coupling capacitances C_b and C_e both lead to the variation of U_{be}. Most daily activities do not change the charges Q_b and Q_e significantly, therefore it is reasonable to attribute the variation of U_{be} mainly to changes in C_b and C_e. Any body movement causes C_b to change. However, C_e may change or remain constant, depending on whether the sensor is attached to a stationary part of the body during daily activities. For instance, eating at a table does not change C_e of an ankle-worn sensor as the leg is almost stationary. Anyway, all body movements cause changes in U_{be} regardless of the location of the sensor on the body.

B. Signal Conditioning Unit

There exist a few preamplifiers capable of converting the electrode signal into a voltage signal [25], which differ in the output waveform, voltage gain, bandwidth, signal-to-noise ratio, etc. A potential amplifier is simply a unit-gain amplifier that converts the high-impedance potential signal of the electrically floating electrode into a low-impedance signal [26]. The parasitic capacitance between the electrode and the local ground plane affects the voltage gain. A trans-resistance amplifier converts the induced current from the electrode into a voltage signal using a resistor placed in the feedback path of an operational amplifier [27]. The magnitude of the output signal is proportional to the rate of change in the target potential. A charge amplifier converts the induced charge on the electrode into a voltage signal using a feedback capacitor [28]. It is immune to parasitic capacitances and its output voltage is proportional to the target potential. Therefore, the charge amplifier is utilized for signal conditioning of the wearable electrostatic sensor.

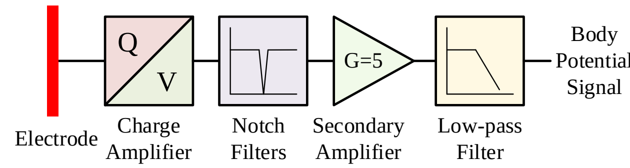

Fig. 4. Block diagram of the signal conditioning unit.

Fig. 3 shows a simplified circuit diagram of the charge amplifier. The electrode for body potential sensing is connected to the inverting terminal of the operational amplifier with ultra-low input bias current. In addition to the feedback capacitor C_f, a large resistor R_f is placed in the feedback path in order to stabilize the DC operating point. Because the electrode is held at the virtual battery ground, the induced charge on the electrode flows through the feedback path and develops the output voltage U_o, which is expressed in phasor representation as

$$U_o = -\frac{j\omega R_f C_{be}}{1 + j\omega R_f C_f} U_{be} \tag{2}$$

If the values of C_f and R_f are chosen to satisfy the condition $\omega R_f C_f \gg 1$, equation (2) is simplified as

$$U_o = -\frac{C_{be}}{C_f} U_{be} \tag{3}$$

It is clear that the feedback capacitor C_f determines the voltage gain of the charge amplifier. The coupling capacitance C_{be} that relies on the permittivity and thickness of the dielectric material between the body and the electrode as well as the size of the electrode also influences the sensitivity of the electrostatic sensor.

The output signal of the charge amplifier is further processed in the signal conditioning unit, as illustrated in Fig. 4. Firstly, two cascaded twin-T notch filters remove the 50 Hz power line noise. Then a secondary amplifier with a voltage gain of 5 boosts the signal to a level suitable for analog-to-digital conversion. Finally, a Butterworth Sallen-Key low-pass filter with a cut-off frequency of 15 Hz is used to filter out high-frequency noise. It should be noted that, although the cut-off frequency of the low-pass filter is lower than the power line frequency, the notch filters are necessary in order to eliminate the strong power line noise. Additionally, the voltage gain of the sensor is so designed that limb and torso movements in daily activities can be detected, such as leg lifting, arm swinging, sitting down and standing up, etc. It is feasible to detect minute movements such as chest movement during breathing by increasing the voltage gain [17], but limb and torso movements would cause saturation of the sensor output.

C. Sensor Development

The wearable electrostatic sensor was designed to be a fully functional smart device capable of sensing, signal conditioning, data processing, wireless communication and data presentation. Fig. 5 shows the prototype and 3D CAD model of the sensing unit. It is embedded in a 3D printed, cylindrical case and can be worn on the wrist, chest or any other part of the body with a band. The bottom of the case separates the electrode from the skin or the cloth. The diameter of the sensor's printed circuit

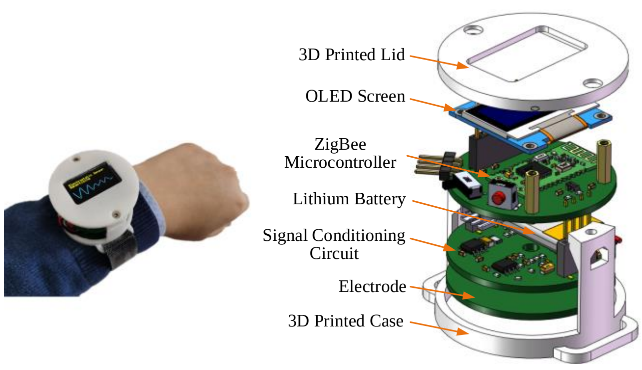

(a) Prototype. (b) 3D CAD model.

Fig. 5. Prototype and 3D CAD model of the wearable electrostatic sensor.

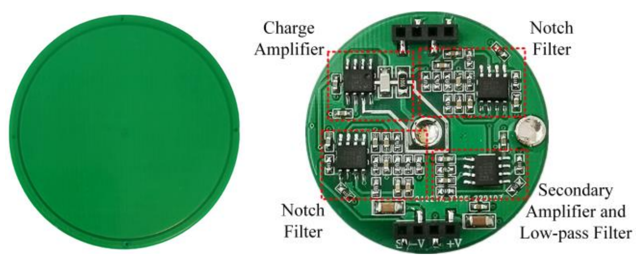

(a) Electrode. (b) Signal conditioning unit.

Fig. 6. Electrode and signal conditioning unit.

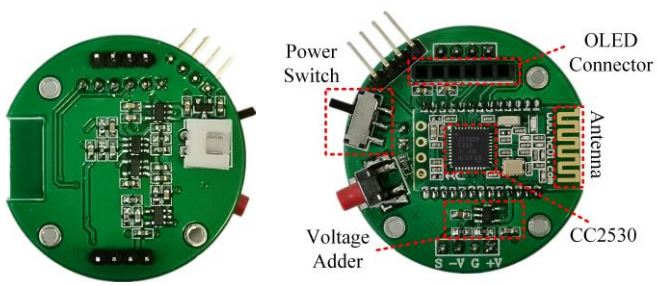

(a) Power circuit. (b) Microcontroller circuit.

Fig. 7. Power and microcontroller circuits.

board (PCB) is 40 mm with an overall height 32 mm due to the stacked structure of the PCBs. It is worth noting that the size of the sensing unit can be easily reduced with custom integrated circuits and MEMS production.

The electrode is an insulated copper disk with a diameter of 36 mm, as shown in Fig. 6(a). In practical applications, exposed conductive electrodes should be avoided, because unexpected touch or sweat on the electrode would affect the signal. The signal conditioning unit is placed on another PCB shown in Fig. 6(b). The two PCBs are soldered back-to-back together, so that the ground planes between the PCBs prevent the electrode signal from being contaminated by the noise in the signal conditioning unit.

The sensor is powered from a rechargeable lithium polymer battery. The 3.7-4.2 V battery voltage is converted into a number of different voltages using the power circuit shown in Fig. 7(a). Because the electrode is held at local ground potential, the amplifiers in the signal conditioning unit operate with $\pm$2.5 V dual power supplies. The digital circuit of the sensor operates with +3.3 V.

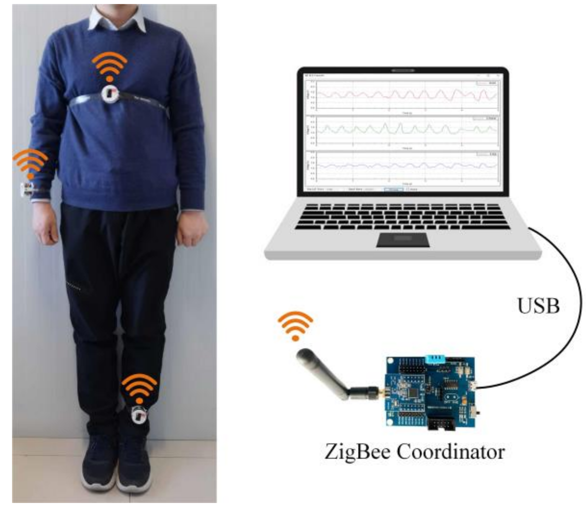

Fig. 8. Experimental setup.

In order to acquire the sensor signal, a wireless microcontroller CC2530 which is designed for ZigBee applications is adopted (Fig. 7(b)). Because the sensor signal can swing between -2.5 V and +2.5 V, a voltage adder is used to shift the signal level to the range of 0 V to +2.5 V in order to match the input range of the Analog to Digital Converter (ADC) of the microcontroller. As a result, the zero baseline voltage of the signal is +1.25 V when no movement is performed. The signal is sampled at a rate of 50 Hz and then displayed on a 0.96-inch OLED screen.

III. Experimental Results and Discussion

A. Experimental Setup

Although the wearable electrostatic sensor can detect limb and torso movements regardless of its mounting location on the body, the pattern and magnitude of the sensor signal depend on its location and motion state. Consequently, experiments were conducted to investigate the influence of the sensor location and type of activity on the sensor signal. To this end, three sensors were developed to collect signals at different body locations simultaneously. It should be stressed that the use of three sensors is not meant to build a WBAN for whole-body movement detection, but to facilitate the investigation into the effect of sensor location on the acquired signal. Additionally, in order to keep consistency of the three sensors, electronic components with high tolerance are adopted.

Fig. 8 shows the experimental setup. The sensors were attached to the left wrist, right ankle and chest of the subject, respectively. The thickness of the cloth between the sensors and the skin is 3 mm, while the cloth fabric is a blend of cotton and polyester. A CC2530 evaluation board configured as Coordinator establishes a ZigBee network and relays the collected signals to a computer through a virtual serial port over a USB cable (Fig. 8). A GUI (graphical user interface) program plots the sensor signals in real time and logs the data for post analysis.

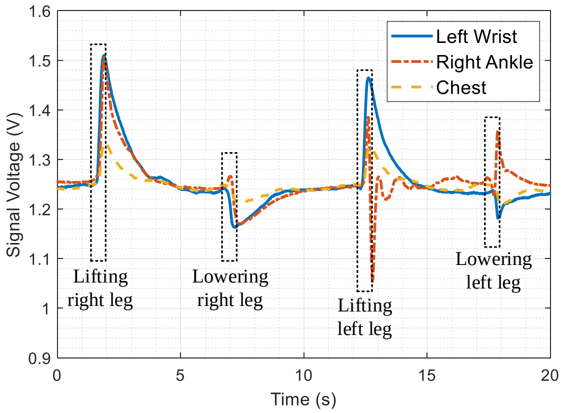

Fig. 9. Sensor signals due to leg lifting and lowering.

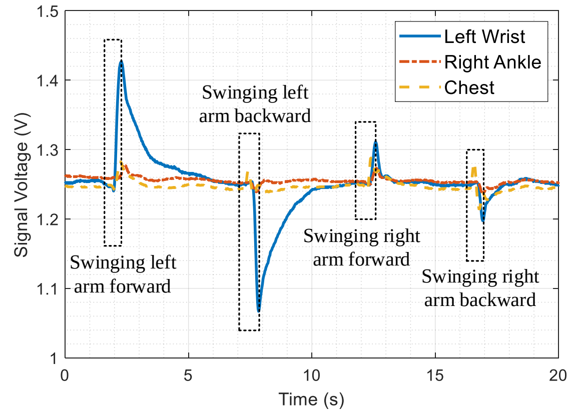

Fig. 10. Sensor signals due to arm swing.

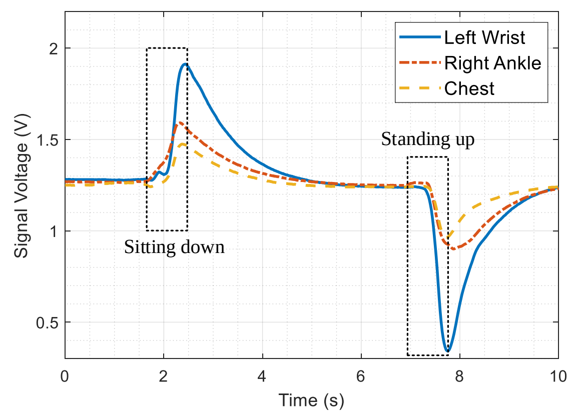

Fig. 11. Sensor signals due to sitting down and standing up.

The experiments started with simple movements, including leg lifting and lowering, arm swing, sitting down and standing up. A temporal correspondence between the movements and the sensor signals was established, which facilitated elucidation of the sensing mechanism. Then, sensor signals due to cyclic daily movements that involve various body elements such as walking and jogging were investigated. Afterwards, the influence of various factors on the signal was experimentally assessed. Finally, the electrostatic sensor was compared with accelerometers for different movements.

B. Sensor Signals of Simple Movements

In the leg lifting and lowering experiment, one foot was raised to a height of 10 cm, held in the air for a few seconds and then lowered back to the floor, while the other parts of the body remained stationary. Fig. 9 plots the sensor signals due to sequentially lifting and lowering the right and left legs. It can be seen that, as the right leg is lifted from 1.4 s to 2.0 s, all sensor signals increase to different peak voltages. When the right leg is held in the air from 2.0 s to 6.6 s, the signals decay gradually to +1.25 V because of the feedback resistor R_f of the charge amplifier that continuously discharges the feedback capacitor C_f. It is noticeable that there are small fluctuations in the decaying signals, because the body cannot stay completely still and the sensors respond to slight body movements. From 6.6 s to 7.3 s, the right foot is lowered to the floor and all sensor signals decrease with different trough voltages. Afterwards, the signals return to +1.25 V gradually.

When the left leg is lifted from 12.1 s to 12.8 s and then lowered from 17.3 s to 17.9 s, the sensor signals from the left wrist and the chest have similar shapes but different magnitudes in comparison with those during moving the right leg, as shown in Fig. 9. However, the pattern of the signal from the right ankle changes substantially. More experiments have confirmed that the approaching and moving away of the left foot relative to the right ankle have caused such changes.

Fig. 10 shows the sensor signals due to sequentially swinging forward and backward the left and right arms. As with the leg moving experiment, all sensors can detect the movements of both arms. In the case of swinging the left arm, the fixation of the sensor on the moving arm produces a strong signal. In general, the signals are weaker than those of moving legs. It can be explained that the stronger capacitive coupling between the feet and the earth ground leads to more significant variation of the body potential when moving legs. It is also clear that the signal from the chest is stronger than that from the ankle because of a closer distance between the chest and the moving arms.

Fig. 11 plots the sensor signals due to sitting down on and standing up from a chair. All sensor signals increase during sitting down and decrease during standing up, both followed by a recovery period when the body is stationary. The signal from the left wrist performing down-and-up movement is stronger than that from the right ankle which is almost stationary. The signal from the chest is the weakest, although the chest also moves during sitting down and standing up.

From the above experiments, the following findings can be summarized regarding the sensing mechanism of the sensor. Firstly, the movements of body parts in opposite directions give rise to opposite changes in the signal voltage. Secondly, mounting of the sensor on a moving body part and a closer distance between the sensor and the moving body part generate a stronger signal. Thirdly, the movement of the foot and the leg that are close to the floor produce a stronger signal than movement of the other parts of the body.

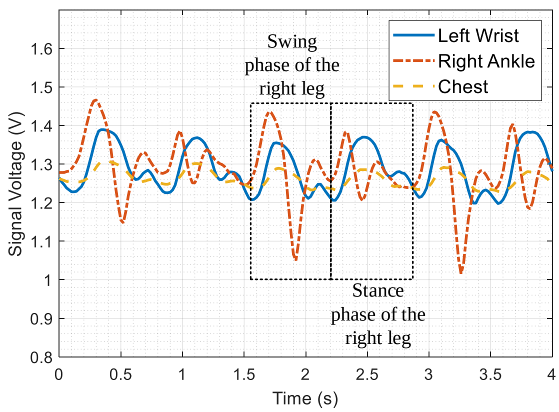

Fig. 12. Sensor signals due to walking.

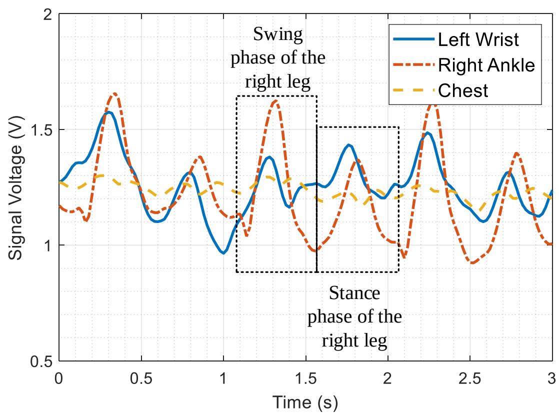

Fig. 13. Sensor signals due to jogging.

C. Sensor Signals of Cyclic Movements

In the walking experiment, the arms swing naturally in an out-of-phase pattern with the legs, i.e. the left arm swings forward when the right leg moves forward, and vice versa for the opposing leg and arm. Fig. 12 shows the sensor signals due to walking. It can be seen that the signals exhibit clear periodicity due to the cyclic nature of the movement. The signal from the right ankle has different patterns during the swing and stance phases of the right leg, whereas the signals from the left wrist and the chest have similar pattern during the two phases. Moreover, the signal from the right ankle has the largest peak magnitude because of the strong capacitive coupling between the feet and the earth ground as well as the large-amplitude movement of the leg. The signal from the chest is the weakest because the torso is relatively stable during walking.

In general, the sensor signals due to jogging (Fig. 13) are stronger than that due to walking because the movement has larger amplitude and faster speed. Roughly, all signals have similar patterns during the swing and stance phases of the right leg. The fundamental frequency of the signals equals the jogging frequency. In addition, the peak magnitude of the signal from the right ankle during the swing phase is larger than that during the stance phase, allowing differentiation between the two phases from the signal.

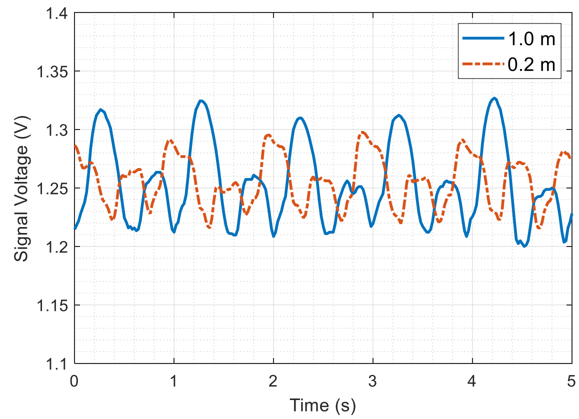

Fig. 14. Sensor signals from the ankle for different distances between the subject and the wall.

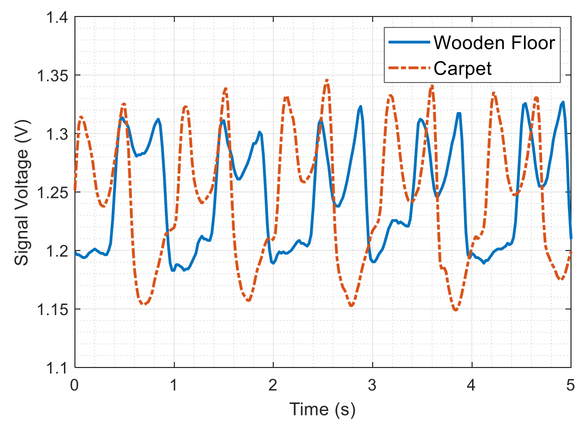

Fig. 15. Sensor signals from the ankle due to walking in place on the wooden floor and the acrylic carpet.

D. Effect of Various Factors

Equation (1) indicates that the electrostatic signal acquired from human activity depends mainly on the coupling capacitance between the human body and the earth ground as well as the amount of charge on the human body, both of which depend on a variety of factors. For instance, the floor, the furniture and appliances in an indoor environment affect the coupling capacitance, while the clothing material, the ambient temperature and humidity affect the charge quantity. The following experiments illustrate the variability of the signal under different conditions.

The influence of the distance between the subject and the wall was investigated with the subject walking in place. Fig. 14 shows the signals from the ankle for distances of 0.2 m and 1.0 m. It can be seen that the signal weakens as the subject gets closer to the wall. Because the wall can be regarded as the earth ground, a closer distance to the wall means larger coupling capacitance between the earth ground and the subject. It follows from equation (1) that the electric potential of the subject is lower and the fluctuation of the sensor signal is weaker (Fig. 14).

The effect of the floor material on the signal of walking in place was then investigated with the subject wearing cotton socks. Fig. 15 exhibits the signals from the ankle due to

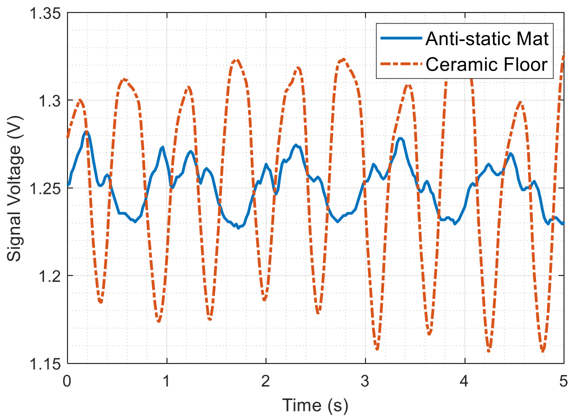

Fig. 16. Sensor signals due to walking in place on an anti-static mat and a ceramic floor.

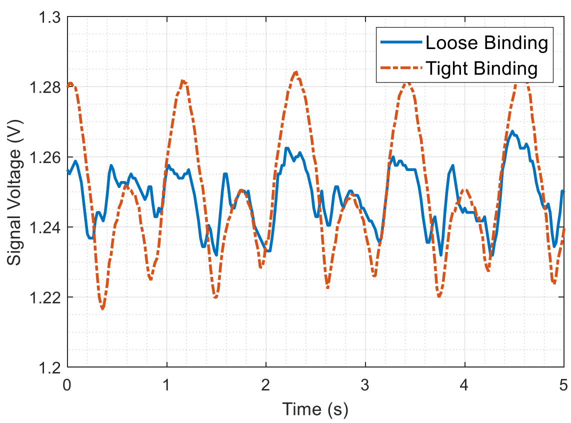

Fig. 17. Sensor signals from the wrist for loose and tight bindings.

walking in place on the wooden floor and the acrylic carpet. As illustrated, the signal for walking on the acrylic carpet is stronger than that for walking on the wooden floor. According to the triboelectric series [29], it is easier for the cotton socks to be charged through friction with the acrylic carpet than with the wooden floor. The stronger signal due to walking on the carpet arises from the larger quantity of charge on the socks.

Anti-static floors are widely seen in industrial workplaces. The effect of the anti-static floor on the sensor signal was experimentally assessed using an anti-static mat with dimensions of 1 m × 1.2 m (width × length). Fig. 16 plots the signals of a wrist-worn sensor due to walking in place on the anti-static mat and a ceramic floor. It can be seen that the magnitude of the signal for the anti-static mat is much smaller than that for the ceramic floor, and the fundamental frequency of the signal for the anti-static mat has reduced by half. The significant effect of the anti-static mat on the sensor signal is explained by its three-layered structure. The top layer of the mat is made of vinyl that is dissipative. The electrostatic charges on the bottom of the shoes are discharged through vinyl. According to equation (1), the potential of the feet is thus significantly reduced. On the other hand, the middle layer of the anti-static mat is a metallic sheet, which functions as an electrostatic screen and reduces the capacitive coupling between the feet and the ground. More experiments have

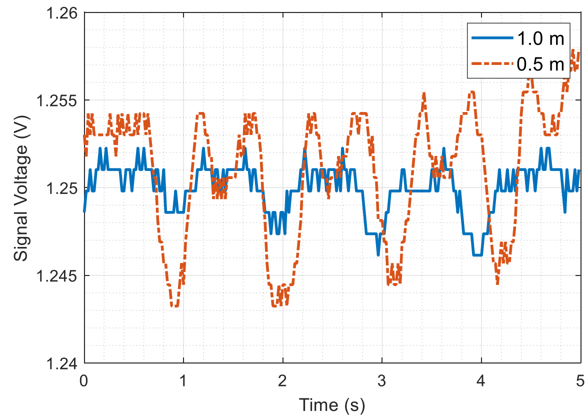

Fig. 18. Sensor signals due to a nearby moving subject.

confirmed that the signal for the anti-static mat is mainly attributed to the swinging of the arm and the leg movement only accounts for the small fluctuations superimposed on the arm swinging signal.

In equation (1), the assumption that the body-electrode capacitance C_{be} remains constant holds when the sensor is firmly attached to the body. However, in practice C_{be} may vary due to loose binding of the sensor and this effect was experimentally assessed. Two sensors were attached to the same wrist for comparison, with one being loosely bound and the other tightly bound. Fig. 17 plots the sensor signals during arm swinging. Because the loosely bound sensor is not as close to the wrist as the tightly bound one, the smaller C_{be} between the loosely bound sensor and the wrist leads to smaller magnitude of the signal. During arm swinging, the loosely bound sensor moves relative to the wrist, which changes C_{be}. Meanwhile, the friction between the sensor and the cloth produces electrostatic charges. As a result, there is obvious noise in the signal from the loosely bound sensor. It is therefore recommended to attach the sensor firmly to the body in order to acquire high-quality signals.

As aforementioned, the electrostatic sensor can work in ambient mode for human activity monitoring, therefore the effect of a nearby moving subject on the sensor signal was experimentally assessed. The sensor was worn on the wrist of a subject standing still while another subject performed walking in place with different distances to the stationary subject. Fig. 18 shows the sensor signals with distances of 1.0 m and 0.5 m, respectively. It can be seen that the electric potential signal of the nearby moving subject is detectable by the sensor worn on the stationary subject, although the magnitude of the signal is much smaller than that due to the subject wearing the sensor. It is also clear that a closer distance leads to a stronger signal. In order to suppress the interference from a nearby subject, the electrostatic sensor should be encased within a metallic box with only the electrode exposed. Because the electrode points toward the body which is a good conductor, the interfering signal can be minimized. It is worth noting that the reason why the waveforms in Fig. 18 are not smooth is because the signal magnitudes are only a bit larger than the resolution of the ADC, which is 1.22 mV.

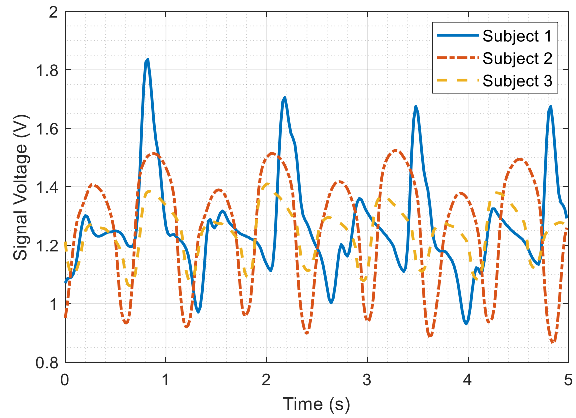

Fig. 19. Sensor signals of three subjects walking in place.

Because the electrostatic sensor is dependent on various factors, it was believed that the signal would vary across subjects. Consequently, three subjects including two males and one female participated in the experiment. The heights of the participants are 187 cm, 170 cm and 157 cm, respectively, whereas their weights are 70 kg, 80 kg and 48 kg, respectively. For the convenience of description, the participants are numbered as 1, 2 and 3. The participants wore different shoes and clothes. The sensor was attached to their left wrists with direct contact with the skin. They performed movements of walking in place with similar stepping frequencies at the same spot in the room. Fig. 19 shows the sensor signals for the three subjects. Although the sensor signal is dependent on various factors, it is clear that the height of the subject has a strong influence on the signal magnitude. Because subject 1 is the tallest and his movement amplitude is the largest, the signal of subject 1 is the strongest. It can also be seen that subjects 2 and 3 have similar signal shapes, but that of subject 1 is apparently different. This could be attributed to the difference in gait between the subjects.

E. Comparison with Accelerometers

Accelerometers are the most common wearable sensors for human activity monitoring. In order to compare with accelerometers, the electrostatic sensor was augmented with a three-axis accelerometer ADXL335, as shown in Fig. 20. The three analog outputs of ADXL335 for accelerations along the X, Y and Z axes were sampled simultaneously with the electrostatic signal.

In the comparative experiment, electrostatic and accelerometer signals were collected from the left wrist and the right ankle of the subject, who performed a series of different movements. Fig. 21 plots the electrostatic signals and the accelerometer outputs along the X axis. For the sake of clarity, the accelerometer outputs along the Y and Z axes are not plotted, as the X axis aligns with the gravity vector in the stationary state and the output is strongest. As shown in Fig. 21, the movements performed during time intervals I-V are lifting and lowering the right leg, lifting and lowering the left leg, swinging both arms in an out-of-phase manner, walking in place, and jogging in place, respectively. During interval I, the accelerometer on the left wrist cannot detect the movement of

Fig. 20. Accelerometer for comparison with the electrostatic sensor.

the right leg, which contrarily can be detected by both electrostatic sensors. During interval II, both accelerometers cannot detect the movement of the left leg, to which both electrostatic sensors can respond. During interval III, the movement of arm swinging is detectable to both electrostatic sensors and the wrist-worn accelerometer only. During intervals IV and V, all sensors can respond to the complex walking and jogging movements. The outputs of the accelerometers are more regular than that of electrostatic sensors which have a more complex sensing mechanism and are affected by various factors. In addition, the mean value of the electrostatic sensor tends to vary because of the large feedback resistor of the charge amplifier that pulls the output slowly to the DC operating point.

F. Discussion

The experimental results demonstrate the feasibility of detecting limb and torso movements using a single wearable electrostatic sensor. This design offers a unique advantage over wearable inertial sensors. The sensor is built with common off-the-shelf components, making it a low-cost option. Power consumption is a critical design parameter of battery-powered wearable sensors [30]. Although the presented design of the sensor is not low-power oriented, it is feasible to achieve power consumption much lower than that of accelerometers using ultra-low power amplifiers available on the market. This sensor has the potential to be deployed in a variety of application scenarios, such as step counting, gait analysis, gaming and entertainment.

Despite the above advantages, there are drawbacks with the wearable electrostatic sensor. The correlation between the signal waveform and the movement pattern is complex, making it difficult to interpret the signal. The strength of the sensor signal is susceptible to the mounting location, height of the human body, and various other factors. It is therefore difficult to measure activity parameters related to the signal strength, such as movement amplitude. For this reason, it is unnecessary to calibrate the sensor for different subjects. Nevertheless, temporal information can be derived from the sensor signal, such as the stepping frequency, number of steps, etc. The above drawbacks pose challenges for application of the sensor in a number of areas, such as recognition of human activity and measurement of physical activity level. Significant future research is required to advance this new sensing technique.

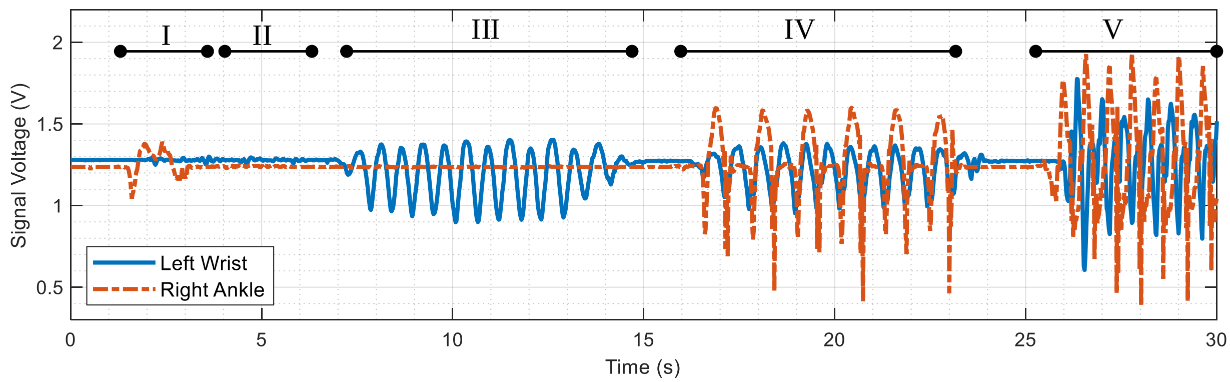

(a) Signals from accelerometers along the X axis.

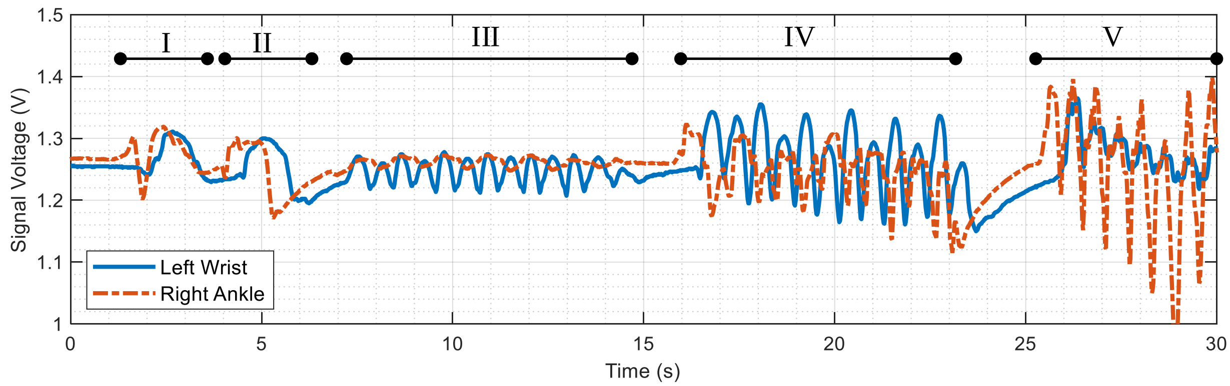

(b) Signals from electrostatic sensors.

Fig. 21. Signals from accelerometers and electrostatic sensors due to different movements. The movements performed during time intervals I-V are lifting and lowering the right leg, lifting and lowering the left leg, swinging both arms in an out-of-phase manner, walking in place, and jogging in place, respectively.

IV. Conclusion

In this paper, a wearable sensor working on the principle of electric field sensing has been developed to monitor human daily activities. The sensing mechanism has been analyzed using an equivalent circuit model. Design and implementation of the sensor have been presented in details. Experimental assessment has been conducted by attaching three prototype sensors to different locations on the subject. Results obtained have demonstrated the capability of the sensor to detect limb and torso movements regardless of its mounting location. The pattern and magnitude of the sensor signal depends on a variety of factors, including mounting location, type of activity, and environmental conditions. Future work will explore the feasibility of the sensor for various motion-sensing applications in real-world scenarios.

References

[1] I. Jeong, D. Bychkov and P. C. Searson, "Wearable devices for precision medicine and health state monitoring," *IEEE Transactions on Biomedical Engineering*, vol. 66, no. 5, pp. 1242-1258, 2019.

[2] A. Singh, S. U. Rehman, S. Yongchareon and P. H. J. Chong, "Sensor technologies for fall detection systems: a review," *IEEE Sensors Journal*, vol. 20, no. 13, pp. 6889-6919, 2020.

[3] M. Rana and V. Mittal, "Wearable sensors for real-time kinematics analysis in sports: a review," *IEEE Sensors Journal*, vol. 21, no. 2, pp. 1187-1207, 2021.

[4] R. Yin, D. Wang, S. Zhao, Z. Lou and G. Shen, "Wearable sensors-enabled human–machine interaction systems: from design to application," *Advanced Functional Materials*, vol. 31, no. 11, Art. no. 2008936, 2021.

[5] M. H. M. Noor, Z. Salcic and K. I. Wang, "Ontology-based sensor fusion activity recognition," *Journal of Ambient Intelligence and Humanized Computing*, vol. 11, pp. 3073-3087, 2020.

[6] M. Javaid, A. Haleem, S. Rab, R. P. Singh and R. Suman, "Sensors for daily life: A review," *Sensors International*, vol. 2, Art. no. 100121, 2021.

[7] M. A. Choukou, A. Polyvyana, Y. Sakamoto and A. Osterreicher, "Ambient assisted living technologies to support older adults' health and wellness: a systematic mapping review," *European Review for Medical and Pharmacological Sciences*, vol. 25, no. 12, pp. 4289-4307, 2021.

[8] P. Picerno, M. Iosa, C. D'Souza, M. G. Benedetti, S. Paolucci and G. Morone, "Wearable inertial sensors for human movement analysis: a five-year update," *Expert Review of Medical Devices*, vol. 18, no. sup1, pp. 79-94, 2021.

[9] F. Lin, A. Wang, Y. Zhuang, M. R. Tomita and W. Xu, "Smart insole: a wearable sensor device for unobtrusive gait monitoring in daily life," *IEEE Transactions on Industrial Informatics*, vol. 12, no. 6, pp. 2281-2291, 2016.

[10] F. S. Botros, A. Phinyomark and E. J. Scheme, "Electromyography-based gesture recognition: is it time to change focus from the forearm to the wrist?" *IEEE Transactions on Industrial Informatics*, vol. 18, no. 1, pp. 174-184, 2022.

[11] Y. Yan, Y. Hu, L. Wang, X. Qian, W. Zhang, K. Reda, J. Wu and Ge Zheng, "Electrostatic sensors - their principles and applications," *Measurement*, vol. 169, Art. no. 108506, 2021.

[12] K. Kurita and S. Morinaga. "Detection technique of individual characteristic appearing in walking motion," *IEEE Access*, vol. 7, pp. 139226-139235, 2019.

[13] K. Kurita and S. Morinaga, "Noncontact detection of movements of standing up from and sitting down on a chair using electrostatic induction," *IEEE Sensors Journal*, vol. 19, no. 19, pp. 8934-8939, 2019.
[14] M. Li, P. Li, S. Tian, K. Tang and X. Chen, "Estimation of temporal gait parameters using a human body electrostatic sensing-based method," *Sensors*, vol. 18, no. 6, Art. no. 1737, 2018.
[15] Y. Kim and C. Moon, "Non-contact gesture recognition using the electric field disturbance for smart device application," *International Journal of Multimedia and Ubiquitous Engineering*, vol. 9, no. 2, pp. 33-140, 2014.
[16] Y. Tang, H. Zhou, X. Sun, N. Diao, J. Wang, B. Zhang, C. Qin, E. Liang and Y. Mao, "Triboelectric touch-free screen sensor for noncontact gesture recognizing," *Advanced Functional Materials*, vol. 30, no. 5, Art. no. 1907893, 2020.
[17] X. Tang and S. Mandal, "Indoor occupancy awareness and localization using passive electric field sensing," *IEEE Transactions on Instrumentation and Measurement*, vol. 68, no. 11, pp. 4535-4549, 2019.
[18] T. Grosse-Puppendahl, X. Dellangnol, C. Hatzfeld, B. Fu, M. Kupnik, A. Kuijper, M. R. Hastall, J. Scott and M. Gruteser, "Platypus - indoor localization and identification through sensing electric potential changes in human bodies," *Proceedings of the 14th Annual International Conference on Mobile Systems, Applications, and Services*, Singapore, 26-30 June 2016, pp. 17-30.
[19] H. Prance, P. Watson, R. J. Prance and S. T. Beardsmore-Rust, "Position and movement sensing at metre standoff distances using ambient electric field," *Measurement Science and Technology*, vol. 23, Art. no. 115101, 2012.
[20] G. Cohn, S. Gupta, T. Lee, D. Morris, J. R. Smith, M. S. Reynolds, D. S. Tan and S. N. Patel, "An ultra-low-power human body motion sensor using static electric field sensing," *Proceedings of the 2012 ACM Conference on Ubiquitous Computing*, Pittsburgh, PA, USA, 5-8 September 2012, pp. 99-102.
[21] A. Pouryazdan, D. Roggen, R. J. Prance and H. Prance, "Wearable electric potential sensing: a new modality sensing hair touch and restless leg movement," *Proceedings of the 2016 ACM International Joint Conference on Pervasive and Ubiquitous Computing*, Heidelberg, Germany, 12-16 September 2016, pp. 846-850.
[22] Y. Sun and X. Yu, "Capacitive biopotential measurement for electrophysiological signal acquisition: a review," *IEEE Sensors Journal*, vol. 16, no. 9, pp. 2832-2853, 2016.
[23] A. Prabakaran and E. Rufus, "Review on the wearable health-care monitoring system with robust motion artifacts reduction techniques," *Sensor Review*, vol. 42, no. 1, pp. 19-38, 2022.
[24] T. Ficker, "Electrification of human body by walking," *Journal of Electrostatics*, vol. 64, no. 1, pp. 10-16, 2006.
[25] Y. Hu, Y. Yan and Y. Yang, "A comparative study of the preamplifiers in electrostatic sensors through analytical modeling and experimental evaluation," *IEEE Transactions on Instrumentation and Measurement*, vol. 71, Art. no. 2004610, 2022.
[26] T. Bednar, B. Babusiak, M. Smondrk, I. Cap and S. Borik, "The impact of active electrode guard layer in capacitive measurements of biosignals," *Measurement*, vol. 171, Art. no. 108740, 2021.
[27] Y. Hu, Y. Yan, L. Wang and X. Qian, "Non-contact vibration monitoring of power transmission belts through electrostatic sensing," *IEEE Sensors Journal*, vol. 16, no. 10, pp. 3541-3550, 2016.
[28] Y. Hu, S. Zhang, Y. Yan, L. Wang, X. Qian and Lu Yang, "A smart electrostatic sensor for online condition monitoring of power transmission belts," *IEEE Transactions on Industrial Electronics*, vol. 64, no. 9, pp. 7313-7322, 2017.
[29] H. Zou, Y. Zhang, L. Guo, P. Wang, X. He, G. Dai, H. Zheng, C. Chen, A. C. Wang, C. Xu and Z. L. Wang, "Quantifying the triboelectric series," *Nature Communications*, vol. 10, Art. no. 1427, 2019.
[30] F. K. Horestani, M. Eshghi and M. Yazdchi, "An ultra-low power amplifier for wearable and implantable electronic devices," *Microelectronic Engineering*, vol. 216, Art. no. 111054, 2019.

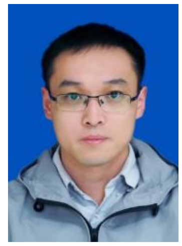

Yonghui Hu (Senior Member, IEEE) received the B.Eng. degree in automation from Beijing Institute of Technology, Beijing, China, in 2004, and the Ph.D. degree in dynamics and control from Peking University, Beijing, in 2009.

He was a Post-Doctoral Research Fellow with Beihang University, Beijing, from 2010 to 2012, and a Research Associate with University of Kent, Canterbury, U.K., from 2019 to 2021. He is currently an Associate Professor with the School of Control and Computer Engineering, North China Electric Power University, Beijing. His current research interests include multiphase flow measurement and condition monitoring of various industrial processes.

Yong Yan (Fellow, IEEE) received the B.Eng. and M.Sc. degrees in instrumentation and control engineering from Tsinghua University, Beijing, China, in 1985 and 1988, respectively, and the Ph.D. degree in flow measurement and instrumentation from the University of Teesside, Middlesbrough, U.K., in 1992.

He was an Assistant Lecturer with Tsinghua University in 1988. In 1989, he joined the University of Teesside as a Research Assistant. After a short period of Post-Doctoral Research, he was a Lecturer with the University of Teesside from 1993 to 1996, and then as a Senior Lecturer, a Reader, and a Professor with the University of Greenwich, Chatham, U.K., from 1996 to 2004. He is currently a Professor of electronic instrumentation and the Director of innovation at the School of Engineering and Digital Arts, the University of Kent, Canterbury, U.K. His current research interests include multiphase flow measurement, combustion instrumentation, and intelligent measurement and condition monitoring.

Dr. Yan was elected as a Fellow of the Royal Academy of Engineering in 2020. He was awarded the gold medal in 2020 by the IEEE TRANSACTIONS ON INSTRUMENTATION AND MEASUREMENT as the most published author of all time from the U.K.